DOI: 10.63527/1607-8829-2025-4-64-75

M.M. Korop[1] (https://orcid.org/0009-0000-4921-3419),
A.V. Prybyla[1] (https://orcid.org/0000-0003-4610-2857),
V.V. Lysko[1,2] (https://orcid.org/0000-0001-7994-6795),
V.H. Pylypko[1] (https://orcid.org/0009-0003-8379-4802),
Yu.B. Khalavka[1] (https://orcid.org/0000-0002-6832-447X)

[1]Yuriy Fedkovych Chernivtsi National University,
2 Kotsiubynskyi str., Chernivtsi, 58012, Ukraine;
[2]Institute of Thermoelectricity of the NAS and MES of Ukraine,
1 Nauky str., Chernivtsi, 58029, Ukraine

Corresponding author: M.M. Korop, e-mail: *koropmykola@gmail.com*

Computer Vision as a Tool for Correlation Analysis of Images of the Microstructure of Bi-Te-Based Thermoelectric Materials

This paper presents the concept of a multimodal computer vision and machine learning tool for establishing correlations between the surface microstructure of extruded Bi-Te-based thermoelectric materials and their thermoelectric properties. The platform integrates data from atomic force microscopy (AFM), metallographic microscopy, chemical composition, thermoelectric properties, and synthesis process conditions into a single database for further deep learning. The developed tool for creating an annotated database, a neural network architecture for automated defect segmentation, and a multimodal data fusion model for predicting thermoelectric properties are described.

Keywords: thermoelectric materials, semiconductors, Bi-Te, artificial intelligence, machine learning, computer vision, defect segmentation, multimodal learning, deep learning, modeling, kinetic coefficients, atomic force microscopy, optical metallographic studies.

Introduction

Bismuth telluride-based thermoelectric materials (TEMs) have attracted considerable research attention due to their ability to convert thermal into electrical energy and vice versa, and are the most efficient materials for low-temperature thermoelectric energy conversion at close to room temperature [1]. The efficiency of these materials is determined by the dimensionless figure of merit *ZT*, for the optimization of which it is necessary to simultaneously increase the power

Citation: M.M. Korop, A.V. Prybyla, V.V. Lysko, V.H. Pylypko, Yu.B. Khalavka (2025). Computer Vision as a Tool for Correlation Analysis of Images of the Microstructure of Bi-Te-Based Thermoelectric Materials. *Journal of Thermoelectricity*, (4), 64–75. https://doi.org/10.63527/1607-8829-2025-4-64-75

factor PF and reduce the thermal conductivity, which are interrelated tasks due to the joint dependence of these parameters on the concentration of charge carriers and the microstructure of the material [2]. The microstructure of extruded TEMs, namely: grain size, grain boundary density, presence of dislocations, nanoprecipitates, and pores, significantly affects the mechanisms of charge and heat transfer [3]. Grain boundaries and point defects scatter phonons, reducing the lattice thermal conductivity κ, while they can negatively affect the charge carrier mobility μ. Therefore, establishing quantitative correlations between microstructural characteristics and functional properties is critically important for intelligent optimization of thermoelectric materials. Over the past decades, there has been no significant improvement in the efficiency of commercially important bismuth telluride-based TEMs due to the complex interplay between the chemical composition, technological synthesis and processing regimes, and microstructure of such alloys. Traditional trial-and-error methods for material optimization are resource-intensive, slow, and poorly scalable. Over the past 5 years, artificial intelligence (AI), machine learning (ML), and computer vision (CV) have become drivers of scientific progress in other classes of materials – steel, ceramics, and composites [4, 5], but such approaches have been practically not applied to Bi-Te-based thermoelectric materials.

The purpose of this work is to present the concept of a comprehensive multimodal system for automated microstructure analysis and prediction of thermoelectric properties of Bi-Te-based TEMs.

1. Literature review

A significant amount of scientific research on the use of ML for AFM-based microstructure analysis is related to extruded Bi-Te-based materials, where processing and synthesis parameters form characteristic microstructural features, which significantly affect the thermoelectric properties of such materials. In the work of Wang et al., a study of hot extrusion of a Bi-Te-Se alloy with Cu doping was conducted and ML models were developed that link extrusion parameters, microstructure characteristics (grain size, phase composition, texture), and Q factor [6]. The authors noted that ML has the potential to reproduce nonlinear dependences between processing conditions and ZT, and can also solve the inverse problem for predicting optimal technological parameters. In subsequent works by Wang et al., the training set for ML was expanded with additional data, namely: extrusion conditions, chemical composition and microstructural characteristics [7]. In further work, the authors further expanded the input data set beyond Cu-doped samples and used ML to identify new technological modes and compositional changes [8].

Although the prediction of properties and optimization of material processing using ML are already well established in thermoelectrics, the application of computer vision to microstructure analysis remains limited, but extremely promising. Sheng et al. developed a synthesis and property analysis process for Cu-Sn-S compounds using ML-based segmentation of their backscattered electron (BSE) micrographs to identify new phases and correlate microstructural features with charge and heat transfer mechanisms [9]. Ling et al. developed methods based on convolutional neural networks and autoencoders that allow compressing

microstructure images to a compact set of parameters and based on them predicting material properties [10]. Pei et al. proposed a "microstructure inversion" approach, in which these parameters can be purposefully changed to design materials with predetermined properties [11]. Such methods, although developed primarily for metals and polymers, can be applied to AFM imaging of thermoelectric materials.

Pręgowska et al. reviewed the application of convolutional neural networks and deep learning algorithms for noise reduction, feature extraction, segmentation, and autonomous scanning in AFM workflows [12]. These methods have the potential to be directly adapted to AFM images of extruded TE materials, enabling the identification of grain boundaries, dislocation lines, domain structures, and nanoprecipitates. Zhang et al. patented an AFM-based device for constructing local Seebeck coefficient distribution maps directly on a sample using a thermal probe [13]. Another patent dedicated to flexible bulk TEMs explicitly envisages the use of AI and ML to optimize the design of a thermoelectric device [14]. These industrial and device developments indicate the promise of research into the relationship between microstructure and thermoelectric properties of TEMs using AFM and machine learning methods.

There are several key trends in the literature supporting the development of AFM-based microstructure analysis using ML for extruded thermoelectric materials. ML for predicting scalar properties has reached maturity but remains largely independent of microstructure image analysis. ML models for the relationship between synthesis and processing technology, microstructure and properties exist for extruded Bi-Te-based systems, but take into account coarse descriptors obtained from traditional microscopy rather than high-resolution imaging.

2. Materials and methods

The objects of the study are extruded TEMs based on Bi-Te of n- and p-type conductivity. Each sample in the database has its own unique identifier, described by the parameters from Table 1 and a set of metadata.

To obtain comprehensive information about the studied sample, a set of complementary research methods is used, which allows to fully assess its characteristics. Fig. 1 presents photographs of the studied samples.

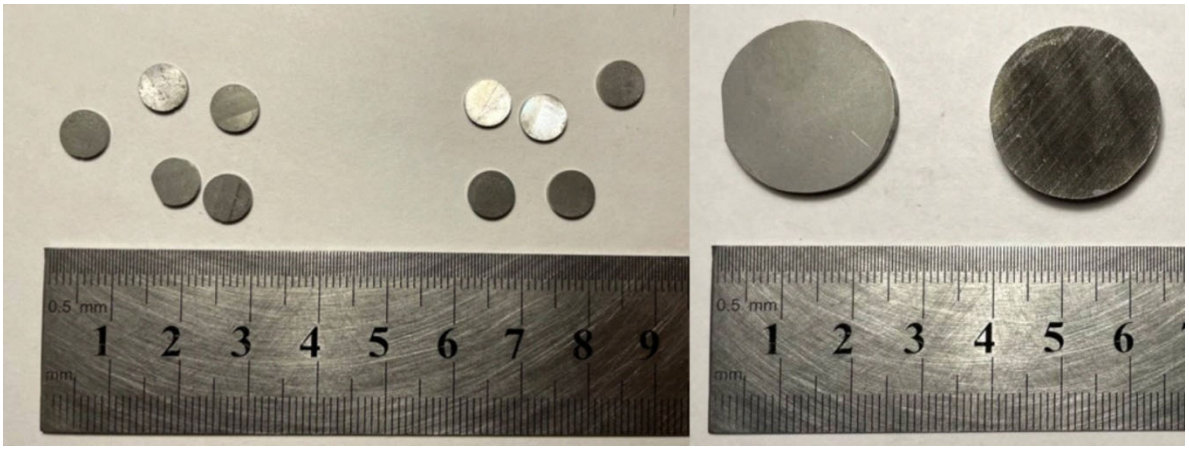

Fig. 1. Photographs of the studied samples of thermoelectric material based on n- and p-type Bi-Te

Table 1

Database structure for storing information about TEM characteristics

Category	**Value in the database**
Chemical composition	Basic matrix composition (Bi, Te, Se, Sb), alloying elements and their concentrations, phase composition (main phase, secondary phases), crystal lattice parameters (*a*, *c*).
Synthesis and processing parameters	Synthesis method, synthesis atmosphere, cooling rate, grinding method of the synthesized TEM, grinding atmosphere, powder granulometric composition, extrusion temperature, pressure, degree of deformation, extrusion direction, lubricant type, annealing temperature and atmosphere, annealing duration, number of heat treatment cycles.
Thermoelectric properties	Seebeck coefficient, electrical conductivity, thermal conductivity κ (total, electronic κ_e, lattice κ), power factor, quality factor *ZT*, temperature dependences *S*(*T*), σ(*T*), κ(*T*), *ZT*(*T*), charge carrier concentration, mobility μ, type of conductivity, anisotropy coefficient.
Microstructural characteristics	Average grain size, grain size distribution, grain aspect ratio, grain boundary type (low angle/high angle), grain boundary density, triple point density, dislocation density, nanoprecipitates (size, density, composition), pores (volume fraction, size), microcracks (length, orientation, type), surface roughness (R_a, R_q).
Microstructure image	AFM: topographic maps, phase maps. Metallography: bright/dark field.
Metadata	Sample ID, manufacturing date, batch number, operator, equipment, measurement date, measurement parameters, sample geometry, sample orientation, surface condition.

Three-dimensional surface topographic maps with nanometer resolution were obtained using the NT-206 AFM in contact mode. The typical scanning parameter was a 46 × 46 μm^2 area with a resolution of 256 × 256 pixels. The initial data were topographic height maps in mps. format from which the roughness parameters were calculated: arithmetic mean roughness, root mean square roughness, fractal dimension of the surface, height distribution and autocorrelation function. Using the SurfaceView program, the obtained microstructure images in Fig. 2 were processed in 2D and 3D modes.

In Figs. 3, 4, TEM surface images were obtained using an optical metallographic microscope in dark field mode with a magnification of 200–400x.

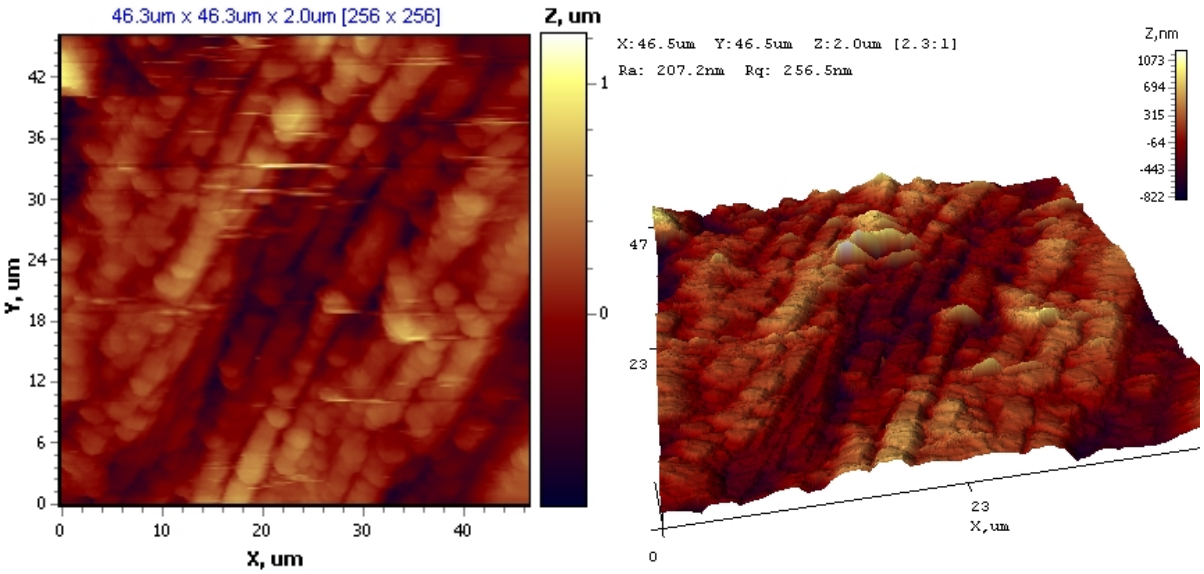

Fig. 2. AFM images of the crystal surface in 2D and 3D mode

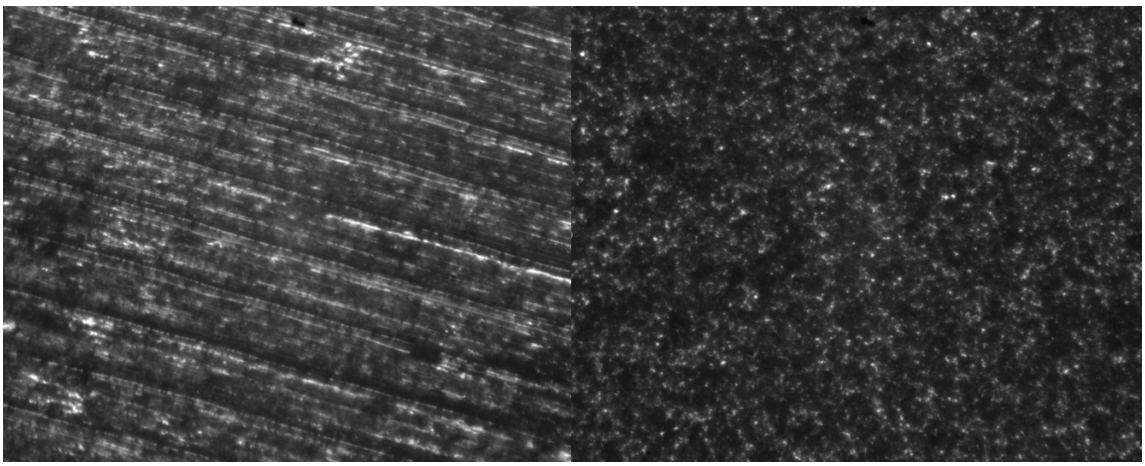

Figs. 3-4. Optical metallographic image of p-type Bi-Te based TEM

ThermoEMF and electrical conductivity measurements are performed using the express "hot probe" method: the sample is placed on a thermostated worktable (with a controlled base temperature), and a heated probe with a built-in thermocouple locally touches the surface and creates a small temperature difference (typically 10–15 K), as a result of which thermoEMF appears in the material, which is recorded relative to the second (fixed) probe and the Seebeck coefficient is calculated using the ratio $\alpha = E/\Delta T$. The coordinate table provides precise positioning of the contact point for measuring distributions across the sample with an accuracy of 0.1 mm. For disks, electrical conductivity is determined by passing a stabilized current through the sample and measuring the voltage drops between coaxial probes in specified configurations, which allows obtaining conductivity components and simultaneously (if necessary) thermoEMF of the central probes with a heater and thermocouples, while all measured values (temperatures, voltages/EMF, coordinates and calculated α and σ) are automatically collected into an automated database on a computer for convenient measurement, further analysis and construction of parameter distribution maps.

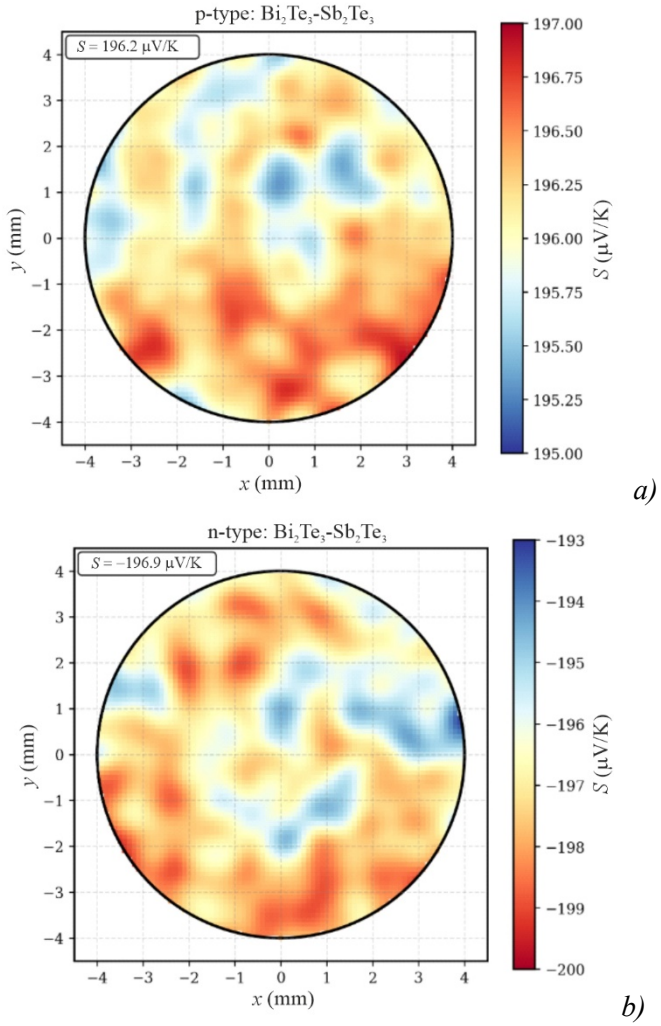

Fig. 5. Map of thermoEMF distribution for a disk of thermoelectric material with p- and n-type conductivity

The key component developed is the ThermoDB Nuclea software tool, which implements a four-step pipeline algorithm for systematically collecting, pre-processing and normalizing, annotating, and linking the obtained data into a multimodal structure. At the first stage, information is imported from various sources, namely: chemical composition, measured thermoelectric properties, AFM and metallographic images, and a record is created in the MySQL database. The second stage involves preprocessing these data for compatibility with ML algorithms: normalization of numerical values, correction of background segmentation for sample selection on metallographic images, plane alignment using the least squares method, and noise filtering for AFM data. For the third stage of annotation, “rough” automatic segmentation methods (Watershed and Otsu) are first used for preliminary marking, which can later be adjusted by an expert using a graphical interface based on LabelMe [15]. The segmentation results of the segmentation masks saved in png. format include: grain matrix, grain boundaries, dislocations, nanoprecipitates, pores, and cracks. The final step in preparing the training dataset involves data argumentation to expand the number of CycleGAN examples [16] and geometric transformations. The training sets contain 80 % training, 15 % validation,

and 5 % test data. The pipeline tool is implemented in Python using the Flask framework with a graphical interface implemented in the Angular framework in Fig. 6.

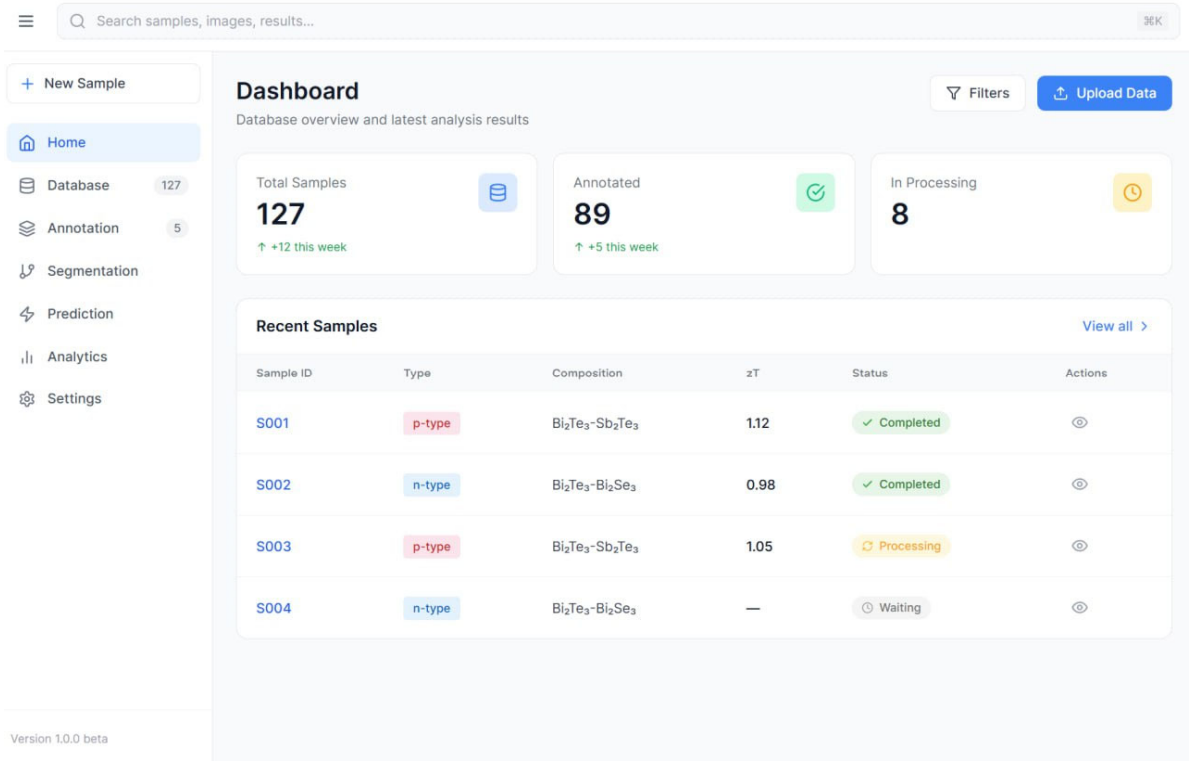

Fig. 6. Graphical interface of the tool for processing, storing and performing TEM analysis

3. Machine learning models for defect segmentation and multimodal property prediction

3.1. Model architecture for semantic segmentation of surface structural features

A specialized software component was developed for segmenting structural features of TEMs on the U-NET encoder-decoder structure [17] with direct (skip) connections. The encoder is created based on the pre-trained ResNet-34 network [18] and consists of 4 blocks with a gradual increase in the number of channels and a decrease in spatial resolution. The first convolutional layer is modified for a single-channel input image by averaging the weights for the three color channels for the trained model. The decoder, in turn, is a symmetric encoder and contains four blocks, including resolution enhancement, direct coupling with encoder features, and convolutional layers. To improve segmentation of small defects, Attention Gates [19] are used to focus attention on relevant areas of the image.

To combine data from different scales, the Feature Pyramid Network (FPN) model [20] is used. This module allows combining features from different decoder levels for a multi-scale representation to improve the detection of large and small surface structures. Additionally, Boundary Class Semantic Segmentation (BCSS) [21] was integrated, which increases the accuracy of grain boundary segmentation, boundary contour prediction, and as a result, through a weighted learning sum, is combined with the segmentation result. To avoid the problem of

fading gradients and stabilize the learning process, additional loss functions are used, which are calculated at intermediate levels of the decoder. As a result, the combined loss function for training the segmentation model is described by formula 1.

$$L_{total} = \lambda_1 L_{CE} + \lambda_2 L_D + \lambda_3 L_B + \lambda_4 L_F \quad (1)$$

where λ_1–λ_4 are weighting factors, L_{CE} is a standard cross-entropy loss function for pixel classification, to measure the difference between predicted class probabilities and true labels, L_D is a function that takes into account class imbalance and calculates the overlap between the predicted and true mask, L_B is a loss function to improve the accuracy of segmentation boundaries and reduce the inaccuracy of object contours, L_F is a loss function to optimize the increase in attention to rare classes and concentration on complex examples [22–23]. 6 segmentation classes were selected: grains, grain boundaries, dislocations, nanoprecipitates of secondary phases, pores and microcracks.

3.2 Multimodal model for predicting properties of thermoelectric materials

The input images are monochrome and single-channel with different resolutions. The AFM image is 256 × 256 × 1 pixels, and represents a topographic height map at the nanoscale. The metallographic microscope has a PixeLINK PL-A741 camera, which allows one to obtain monochrome images of the surface microstructure. Since both image types are single-channel and depict microstructure at different scales, a shared-weights architecture is used. Both image streams are processed by a single ResNet-34 encoder. Metallographic images are pre-scaled to 256 × 256 pixels while preserving the aspect ratio by cropping the image with the base in the center. The first convolutional layer is modified for single-channel input by averaging the weights, dividing by 3. The output global feature vector has dimension 1792, which is reduced to 256 through a dense layer with normalization and ReLU activation. The result is the latent representations $Z_{afm}(R^{256})$ and $Z_{met}(R^{256})$. Additional information about the chemical composition, technological parameters of synthesis and processing are processed by a multilayer neural network in the form of input parameters, 64 neurons, 128 neurons and an output layer of 128 neurons. Each layer of this network includes BatchNorm normalization and ReLU activation function. The initial latent representation of Z_{data} (R^{128}). To generalize the model of relationships between modalities, a cross-modal attention mechanism based on the Transformer [24] is used. The combination of Z_{met} and Z_{data} is used as the key and value of the "answers" from metallographic data and information on chemical composition and technological modes. The mechanism of "multi-headed attention" (4 heads) simultaneously tracks different types of relationships between modalities and produces a vector of 512 features containing information from all sources. The final merging of modalities is carried out through an adaptive model with weights α, β, γ for each modality according to formula 2:

$$Z = \alpha Z_{afm} + \beta Z_{met} + \gamma Z_{data} \quad (2)$$

The weights are normalized using the softmax formula ($\alpha + \beta + \gamma = 1$) and trained together with the rest of the network to allow the model to automatically determine the importance of each specific modality for predicting a specific property. Contrastive learning is used to improve the alignment of representations of the same sample from different modalities [25].

Positive pairs are formed from Z_{afm}, Z_{met} of the same sample so that the vectors are close in the latent space, respectively, negative pairs are formed from different samples so that the vectors are distant. A contrast component InfoNCE is added to the general loss function, which teaches the model to bring together vectors of the same sample from different sources and to repel vectors of different samples. This increases the robustness of the model when one of the data sources is missing. For each predicted property (Seebeck coefficient, electrical conductivity, thermal conductivity, power factor, quality factor) a separate regression head is used with a structure of 256 input neurons, 128 and 64 respectively for hidden layers per 1 neuron in the output layer. All these properties are predicted in parallel. This allows the model to learn the specific dependence of each property on the microstructure. A loss function based on the mean square error is used during model training, with the ability to adapt depending on the importance of the feature.

To ensure the interpretability of the predictions, the Grad-CAM image region visualization technique [26] is used, which allows generating a heat map, where areas with high and low influence are displayed in different colors, to check the accuracy of the model [27]. Additionally, the analysis of the modality weights allows to establish which of them is the most important for a particular property. The implementation of the platform has the potential to provide a deeper understanding of the physical mechanisms of the influence of microstructure on transport properties, as well as to provide a practical tool for accelerated optimization of thermoelectric materials.

Conclusions

1) The concept of a tool for a comprehensive multimodal analysis system for establishing correlations between structure and thermoelectric properties is presented and its detailed description is provided. The platform includes three key components: a tool for creating an annotated database with systematic linking of images, composition and properties, a neural network architecture for automated segmentation of microstructural defects, and a multimodal model with shared encoder weights for predicting thermoelectric properties based on the fusion of monochrome images of different resolutions with data on chemical composition and technological synthesis modes.
2) The first annotated database of thermoelectric materials was created by combining AFM and metallographic images of extruded Bi-Te-based thermoelectric materials.
3) The proposed tool allows one to reduce the time for analyzing a material sample by 1–2 orders of magnitude compared to the manual method.

Authors' information

M.M. Korop – Postgraduate student of the Department of Thermoelectricity and Medical Physics of the Yu. Fedkovych National University of Chernivtsi, junior researcher of the Institute of Thermoelectricity of the NAS and MES of Ukraine.
A.V. Prybyla – Candidate of Physical and Mathematical Sciences, Assistant Professor of the

Department of Thermoelectricity and Medical Physics, Yu. Fedkovych National University of Chernivtsi.
V.V. Lysko – Candidate of Physical and Mathematical Sciences, Acting Director of the Institute of Thermoelectricity.
V.H. Pylypko – Doctor of Philosophy, Head of the laboratory of the Research Center "Functional Materials Technology", Educational and Research Institute of Biology, Chemistry and Bioresources, Yu. Fedkovych National University of Chernivtsi.
Yu.B. Khalavka – Doctor of Chemical Sciences, Associate Professor Vice-Rector for Scientific Work of the Yu. Fedkovych National University of Chernivtsi.

References

1. Snyder G.J., & Toberer E. S. (2008). Complex thermoelectric materials. *Nature Materials*, 7(2), 105–114. https://doi.org/10.1038/nmat2090
2. Pei Y., Shi X., LaLonde A., Wang H., Chen L., & Snyder G. J. (2011). Convergence of electronic bands for high performance bulk thermoelectrics. *Nature*, 473(7345), 66–69. https://doi.org/10.1038/nature09996
3. Kim S. I., Lee K. H., Mun H. A., Kim H. S., Hwang S. W., Roh J. W., Yang D. J., Shin W. H., Li X. S., Lee Y. H., Snyder G. J., & Kim S. W. (2015). Dense dislocation arrays embedded in grain boundaries for high-performance bulk thermoelectrics. *Science*, 348(6230), 109–114. https://doi.org/10.1126/science.aaa4166
4. DeCost B. L., & Holm E. A. (2015). A computer vision approach for automated analysis and classification of microstructural image data. *Computational Materials Science*, 110, 126–133. https://doi.org/10.1016/j.commatsci.2015.08.011
5. Azimi S. M., Britz D., Engstler M., Fritz M., & Mücklich F. (2018). Advanced steel microstructural classification by deep learning methods. *Scientific Reports*, 8(1). https://doi.org/10.1038/s41598-018-20037-5
6. Wang Z., Yokoyama Y., Onda T., Adachi Y., & Chen Z. (2019). Improved thermoelectric properties of hot-extruded Bi–Te–Se bulk materials with Cu doping and property predictions via machine learning. *Advanced Electronic Materials*, 5(6). https://doi.org/10.1002/aelm.201900079
7. Wang Z., Adachi Y., & Chen Z. (2019). Processing optimization and property predictions of hot-extruded Bi-Te-Se thermoelectric materials via machine learning. *Advanced Theory and Simulations*, 3(1). https://doi.org/10.1002/adts.201900197
8. Wang Z.-L., Funada T., Onda T., & Chen Z.-C. (2023). Knowledge extraction and performance improvement of Bi2Te3-based thermoelectric materials by machine learning. *Materials Today Physics*, 31, 100971. https://doi.org/10.1016/j.mtphys.2023.100971
9. Sheng Y., Deng T., Qiu P., Shi X., Xi J., Han Y., & Yang J. (2021). Accelerating the discovery of Cu–Sn–S thermoelectric compounds via high-throughput synthesis, characterization, and machine learning-assisted image analysis. *Chemistry of Materials*, 33(17), 6918–6924. https://doi.org/10.1021/acs.chemmater.1c01856
10. Ling J., Hutchinson M., Antono E., DeCost B., Holm E. A., & Meredig B. (2017). Building

data-driven models with microstructural images: generalization and interpretability (Version 1). arXiv. https://doi.org/10.48550/ARXIV.1711.00404

11. Pei Z., Rozman K. A., Doğan Ö. N., Wen Y., Gao N., Holm E. A., Hawk J. A., Alman D. E., & Gao M. C. (2021). Machine-learning microstructure for inverse material design. *Advanced Science*, 8(23). https://doi.org/10.1002/advs.202101207
12. Pregowska A., Roszkiewicz A., Osial M., & Giersig M. (2024). How scanning probe microscopy can be supported by Artificial Intelligence and quantum computing (Version 1). arXiv. https://doi.org/10.48550/ARXIV.2406.19397
13. Zhang X., et al. (2013). Nano-thermoelectric Seebeck coefficient in-situ quantitative characterization device based on AFM. *WO Patent WO201318911 1A1*.
14. Moon, J., et al. (2021). Compliant three-dimensional thermoelectrics. *US Patent US2021017540 6A1.*
15. Russell B. C., Torralba A., Murphy K. P., & Freeman W. T. (2007). LabelMe: A database and Web-based tool for image annotation. *International Journal of Computer Vision*, 77(1–3), 157–173. https://doi.org/10.1007/s11263-007-0090-8
16. Zhu J.-Y., Park T., Isola P., & Efros A. A. (2017). Unpaired image-to-image translation using cycle-consistent adversarial networks (Version 7). arXiv. https://doi.org/10.48550/ARXIV.1703.10593
17. Ronneberger O., Fischer P., & Brox T. (2015). U-Net: convolutional networks for biomedical image segmentation (Version 1). arXiv. https://doi.org/10.48550/ARXIV.1505.04597
18. He K., Zhang, X. Ren S., & Sun J. (2015). Deep residual learning for image recognition (Version 1). arXiv. https://doi.org/10.48550/ARXIV.1512.03385
19. Oktay O., Schlemper J., Folgoc L. L., Lee M., Heinrich M., Misawa K., Mori K., McDonagh S., Hammerla N. Y., Kainz B., Glocker B., & Rueckert D. (2018). Attention U-Net: learning where to look for the pancreas (Version 3). arXiv. https://doi.org/10.48550/ARXIV.1804.03999
20. Lin T.-Y., Dollar P., Girshick R., He K., Hariharan B., & Belongie S. (2017). Feature pyramid networks for object detection. In 2017 IEEE Conference on Computer Vision and Pattern Recognition (CVPR) (pp. 936–944). *2017 IEEE Conference on Computer Vision and Pattern Recognition (CVPR). IEEE.* https://doi.org/10.1109/cvpr.2017.106
21. Fotos G., Campbell A., Murray P., & Yakushina E. (2023). Deep learning enhanced Watershed for microstructural analysis using a boundary class semantic segmentation. *Journal of Materials Science*, 58(36), 14390–14410. https://doi.org/10.1007/s10853-023-08901-w
22. Sudre C. H., Li W., Vercauteren T., Ourselin S., & Cardoso M. J. (2017). Generalised Dice overlap as a deep learning loss function for highly unbalanced segmentations. arXiv. https://doi.org/10.48550/ARXIV.1707.03237
23. Lin T.-Y., Goyal P., Girshick R., He K., & Dollar P. (2017). Focal loss for dense object detection. In 2017 IEEE International Conference on Computer Vision (ICCV) (pp. 2999–3007). *2017 IEEE International Conference on Computer Vision (ICCV). IEEE.*

https://doi.org/10.1109/iccv.2017.324
24. Yaslioglu M. M. (2025). Attention is all you need until you need retention (Version 1). arXiv. https://doi.org/10.48550/ARXIV.2501.09166
25. Chen T., Kornblith S., Norouzi M., & Hinton G. (2020). A simple framework for contrastive learning of visual representations (Version 3). arXiv. https://doi.org/10.48550/ARXIV.2002.05709
26. Selvaraju R. R., Cogswell M., Das A., Vedantam R., Parikh D., & Batra D. (2016). Grad-CAM: Visual explanations from deep networks via gradient-based localization. arXiv. https://doi.org/10.48550/ARXIV.1610.02391
27. Lundberg S., & Lee S.-I. (2017). A unified approach to interpreting model predictions (Version 2). arXiv. https://doi.org/10.48550/ARXIV.1705.07874

Submitted: 15.12.25

Короп М.М.[1] (https://orcid.org/0009-0000-4921-3419),
Прибила А.В.[1] (https://orcid.org/0000-0003-4610-2857),
Лисько В.В.[1,2] (https://orcid.org/0000-0001-7994-6795),
Пилипко В.Г.[1] (https://orcid.org/0009-0003-8379-4802),
Халавка Ю.Б.[1] (https://orcid.org/0000-0002-6832-447X)

[1]Чернівецький національний університет, ім. Юрія Федьковича,
вул. Коцюбинського, 2, Чернівці, 58012, Україна;
[2]Інститут термоелектрики НАН і МОН України,
вул. Науки, 1, Чернівці, 58029, Україна

Комп’ютерний зір як інструмент кореляційного аналізу зображень мікроструктури термоелектричних матеріалів на основі Bi-Te

У даній роботі представлено концепцію інструмента мультимодальної системи комп'ютерного зору та машинного навчання для встановлення кореляцій між мікроструктурою поверхні екструдованих термоелектричних матеріалів на основі Bi-Te та їхніми термоелектричними властивостями. Платформа поєднує дані атомно-силової мікроскопії (АСМ), металографічної мікроскопії, хімічного складу, термоелектричних властивостей та технологічних режимів синтезу у єдину базу для подальшого глибокого навчання. Описано розроблений інструмент для створення анотованої бази даних, архітектуру нейронної мережі для автоматизованої сегментації дефектів, а також мультимодальну модель поєднання даних для прогнозування термоелектричних властивостей.

Ключові слова: термоелектричні матеріали, напівпровідники, Bi-Te, штучний інтелект, машинне навчання, комп'ютерний зір, сегментація дефектів, мультимодальне навчання, глибоке навчання, моделювання, кінетичні коефіцієнти, атомно-силова мікроскопія, оптичні металографічні дослідження.

Надійшла до редакції 15.12.25